

Chapter 24

In Vitro Three-Dimensional Cancer Culture Models

Waseem Asghar, Hadi Shafiee, Pu Chen, Savas Tasoglu, Sinan Guven, Umut Atakan Gurkan, and Utkan Demirci

Abstract The efficacy of chemotherapy drug candidates is conventionally investigated using 2D cancer cell cultures and in vivo animal models. It is crucial to determine signaling pathways, controlling cell proliferation, metabolism, differentiation, and apoptosis functions, which are not optimal to investigate in the monolayer 2D cell culture models. Further, accurate investigation of tumor growth and therapeutic drug efficacy in murine models is challenging because of technical constraints of in vivo imaging and requires euthanizing the animals. Therefore, alternative in vitro cancer models are needed to facilitate the transition of new chemotherapeutic drug candidates from bench to clinical trials. Recent technological advances in microfabrication and bioengineering have provided tools to develop in vitro 3D cancer models that mimic natural tissue microenvironment. This chapter highlights recent developments in in vitro 3D cancer models and their applications for studying the efficacy of the chemotherapeutic drug candidates. We discuss the

Waseem Asghar and Hadi Shafiee contributed equally to this work.

W. Asghar • H. Shafiee • P. Chen • S. Tasoglu • S. Guven
Bio-Acoustic-MEMS in Medicine (BAMM) Laboratory, Center for Biomedical Engineering,
Department of Medicine, Brigham and Women's Hospital, Harvard Medical School,
Cambridge, MA, USA

U.A. Gurkan
CASE Biomufacturing and Microfabrication Laboratory (CASE-BML),
Department of Mechanical and Aerospace Engineering,
Advanced Platform Technology Center, Louis Stokes Cleveland Veterans
Affairs Medical Center, Case Western Reserve University,
Cleveland, OH, USA

U. Demirci (✉)
Bio-Acoustic-MEMS in Medicine (BAMM) Laboratory, Center for Biomedical Engineering
and Division of Infectious Diseases, Brigham and Women's Hospital, Harvard Medical
School, Cambridge, MA, USA

Harvard-MIT Health Sciences and Technology, Cambridge, MA, USA
e-mail: udemirci@rics.bwh.harvard.edu

methods and technologies to develop 3D cancer models including embedded and overlay cell culture, suspension culture, bioprinting, hanging drop, microgravity bioreactor, and magnetic levitation. We also discuss the extracellular matrix components and synthetic scaffolds used in vitro 3D cancer models.

Introduction

Cancer caused 7.6 million deaths worldwide in 2008 [1]. About 80 % of tumors are originated from the epithelium characterized by the uncontrolled growth of epithelial cells [2]. Epithelial cells interact with other cells like endothelial and stromal fibroblast cells, and extracellular matrix (ECM) based on microenvironmental conditions [2, 3]. Endothelial vasculature provides oxygen and nutrients to other cells present in ECM. This vasculature also provides the immune system cells (macrophages, neutrophils and mast cells) to fight against pathogens and for removal of dead cells. ECM consists of a mesh of protein fibers like elastins and collagens [4]. The fibers are further functionalized with cell adhesive proteins such as fibronectin and laminin. These cell adhesive proteins on ECM provide binding locations for the cells to get attached to ECM through cell transmembrane integrin receptors. In blood cells, the integrins also mediate cell–cell adhesion along with ECM adhesion. All of these receptors are involved in intracellular signaling pathways and regulate cell growth, shape, proliferation, migration and differentiation [4]. Occasionally cell signaling pathways are disturbed (e.g., due to injury) that results into the proliferation and movement of epithelial sheets. These abnormal conditions are reversible upon healing. If the inflammable conditions are sustained, the stromal fibroblast and macrophages continuously upregulate the matrix metalloproteinase (MMP) enzymes that remodel ECM and can promote abnormal cell proliferation [2]. Abnormal cell interactions and signaling pathways can lead to genetic mutations, and hence epithelial cells attain tumorigenic potential [5]. At this stage, the cancer cells behave as an independent organ and define their cellular responses and reorganize ECM to accommodate tumor mass formation. The tumor size cannot grow beyond 200 μm without the nutrients and oxygen supply that induce the upregulation of hypoxia-inducible factor (HIF1 α) [6]. Hypoxia leads to a signaling cascade followed by upregulation of angiogenic growth factors including vascular endothelial growth factor (VEGF). New blood vessels are formed in response to these changes that can supply nutrients and oxygen to growing tumor cells. Tumor aggressiveness is further enhanced by the increased secretion of other growth factors such as basic fibroblast growth factor (bFGF) and interleukin-8 (IL-8) [7]. As a result, the cancer grows continuously into a solid tumor along with the supporting vasculature and microenvironment.

Many chemotherapeutic drugs have been introduced to treat cancer. Most of these drugs fail during transition from murine models to clinical trials [8]. On the other hand, the number of potential drugs waiting to be tested far exceeds the number of patients available for drug testing. Therefore, alternative in vitro cancer models for verification and testing of drugs are needed [9]. Conventionally, 2D cancer cell culture and in vivo

animal models are used to determine the efficacy of chemotherapeutics. Both of these models have certain advantages and limitations. In 2D cell culture techniques, the cancer cells are cultured on the plastic substrata as a monolayer where important signaling pathways controlling cell proliferation, metabolism, differentiation, and apoptosis functions are lost; whereas in natural form the cancer cells grow into 3D tumor mass while interacting with other cells and the ECM. For instance, when breast cancer cells were cultured on 2D substrata and treated with various signaling inhibitors, there was no change in expression and activity of β 1-integrin and epidermal growth factor receptors (EGFR); whereas these activities were reciprocally down regulated when cancer cells were cultured in 3D tumor model [10]. In another report, tumor cells were treated with PI3-Kinase inhibitors in both 2D and 3D tumor culture models. The inhibitors mediated the reversion of malignant phenotype only in 3D tumor model by down regulation of EGFR and β 1-integrin whereas in 2D tumor culture, these phenomena were absent [11]. The 2D cancer cultures respond differently to exogenous apoptotic stimuli and chemotherapeutic agents. Tumor cells cultured in 3D spheroids attained multidrug resistance phenotype when exposed to a chemotherapeutic agent whereas cancer cells cultured on 2D substrata were sensitive to drug treatment [12, 13]. These results implied that the composition of tissue ECM and cell–ECM interactions generated resistance to apoptosis, a phenomena absent in 2D monolayer cultures [13–15]. Solid tumors such as breast and liver cancers are denser and hypoxic at the center, which cannot be modeled using the 2D culture technique that includes just a monolayer of cells. Therefore, it is obvious that 2D cancer culture models present limitations in providing a natural 3D microenvironment for cancer cells and may not be effective to study the drug efficiency.

The human tumor xenograft model is the most commonly used *in vivo* tumor model that can provide natural 3D tumor microenvironments. In this method, small cancerous tissue biopsies or inoculating cancer cells are placed either subcutaneously or into the other organs of immunocompromised mouse and allowed to proliferate for couple of weeks [16, 17]. Mice used in this model are immunocompromised and therefore the injected human cancer cells are not rejected. Different types of immunocompromised mice are available for xenograft models including athymic nude mice, severely compromised immunodeficient (SCID) mice and non-obese diabetic (NOD) SCID mice [17–20]. Although the xenograft mice models can induce the immune response similar to native tumor stroma, the imaging of tumor growth after specific time intervals is very challenging. The drug efficacy can only be analyzed when the mouse is sacrificed at the end. Although the modern *in vivo* imaging systems can be used to assess the drug efficacy during experiment, these imaging systems are costly [21–24]. Previously, xenograft mice models were used to test the efficacy of angiogenic inhibitor endostatin [25, 26]. It was concluded that tumor regressed effectively once treated with endostatin. The later clinical trials revealed that endostatin interacted differently in humans; only 20 % of the patients administrated with endostatin showed tumor regression, while no toxicity was observed in any patients [27]. Although xenograft mice models are preferable to 2D cancer culture models, they can, sometimes, lead to false interpretations. Therefore, there is an unmet need to develop *in vitro* 3D cancer culture models that employ human cells and which can reliably recapitulate native tissue structures.

In vitro 3D cancer models rely on encapsulating cells within hydrogels or scaffolds or seed them on a defined substrate and method where they can form 3D aggregates mimicking natural tissue microenvironments while overcoming some of the limitations of 2D and xenograft animal models. 3D cancer models can be composed of single or multiple cell types. This chapter focuses on the state-of-art technologies and processes that were developed for 3D cancer cultures and cocultures. Most of the in vitro 3D cancer models have been introduced including spheroids, hanging drop cell encapsulation and printing, and scaffold seeding. Further, the effects of dynamic fluid flow conditions and scaffold stiffness on cancer growth are discussed. In the end, future research directions are also described.

Methods and Technologies to Develop 3D Cancer Models

Recapitulating in vivo metabolic activities and spatial organization of cells within in vitro conditions hold paramount assets in cancer research. In vitro culture models mimicking features of native environments are in great importance in order to reveal cancer cell activities including self-sustained growth signal secretion, resistance and insensitivity to inhibitory cytokines, avoidance of apoptosis, continuous self-division, angiogenesis, migratory capacity, and metastasis [28]. Native tissue environment provides co-localization of different cell types in a well-defined organization enhancing cell–cell contact, exchange of secreted signaling cytokines and cell–ECM interactions [29]. Coculture of relevant cell types enhances cell–cell cross talk through secreted cytokines and growth factors. External addition of growth factors lacks in dose precision and timing. Such cross talk between cell types can be implemented simply by seeding multiple cell types together simultaneously in the same place or by introducing particular cell type on top of the pre-seeded cell layer (i.e., fibroblast cells). In such methods, cells have direct cell–cell interactions and different cell types can be plated in cell culture inserts. Such inserts have porous membranes that provide the exchange of cytokines between cells. Indirect cell–cell cross talk can also be established by obtaining a conditioned culture media from one cell type or culture time point and using it in another cell culture or time point. Classical monolayer cell cultures are able to assist needs to coculture multiple cell types and supply signaling cytokines by introducing them through culture media. However, spatial organization of cell morphology and interpretation of physical and biochemical cues from ECM are unmet.

Embedded and Overlay Cell Cultures

Efforts to mimic native microenvironment introduced basic ingredients of ECM such as collagen type I, collagen type IV, fibronectin, laminin and glycosaminoglycans, and elastin as tools to build a basement membrane in 3D culture systems

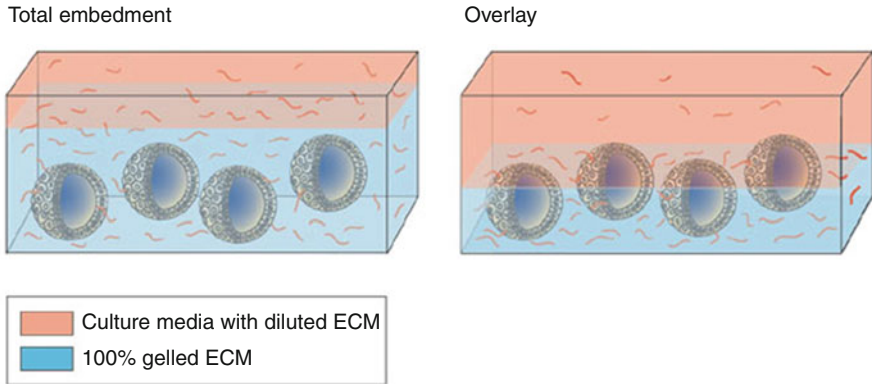


Fig. 24.1 Schematic representation of embedded and overlay culture models. Reprinted by permission from Macmillan Publishers Ltd: [NATURE REVIEWS CANCER], copyright (2005) [169]

including Matrigel™ and alginate based materials [30]. Basement membrane can be applied in two different ways to promote 3D cellular organizations: (1) embedded, and (2) overlay culture. Both methods aim to establish biologically relevant contact between cells and substratum. In the embedding method, cells are suspended into the basement membrane and applied in culture well (Fig. 24.1 left). Encapsulated cells start to adhere, reshape and secrete factors (e.g., MMP) to remodel the matrix that provide space for spreading, proliferation and migration to contact other cells [31]. In an overlay culture, basement membrane is applied to the surface of a substrate and forms a thin hydrogel coating. Later, cells are introduced with culture media on the coating (Fig. 24.1 right). Formation of the optimum 3D cell organizations depends on the type of applied cells and basement membranes. Some cell types require additional biological cues from the basement membrane such as growth factors. For instance, most of the epithelial cells form spherical hollow cysts only when embedded in Matrigel™, whereas Madin-Darby canine kidney (MDCK) epithelial cells can easily develop into polarized cell clusters with a hollow lumen when encapsulated within collagen type I hydrogels [32, 33].

Suspension Culture

3D cell cultures can also be achieved by culturing cells in suspension. In this method, cell adhesion to the substratum of culture plate is reduced or prevented. Regular cell culture plates are made of polystyrene and have treated surfaces that provide negatively charged hydrophilic properties enhancing cell adhesion. When there is no treatment applied, polystyrene surfaces are uncharged and have hydrophobic nature, which results in poor and uneven cell adhesion. Cell adhesion decreases dramatically by 99.8 % when special treatment is applied to polystyrene

surface by making it neutral and still hydrophilic (Corning Ultra-Low Attachment Surface). Alternatively, agarose coated cell culture plates also provide suspension culture conditions.

Hanging Drop Technique

In standard cell culture, cells are pressed against hard flat surfaces by gravitational force, which results in constrained cell growth in a two-dimensional plane. Hanging drop technique allows to gravitationally aggregate cells at a flexible, spherical air–liquid interface within hanging drops, which facilitates the formation of 3D cell structure (e.g., spheroids) without a scaffold [34–37]. Currently, a number of commercial 3D cell culture products are available in market based on hanging drop technique (Table 24.1). For example, InSphero Company offers GravityPLUS™ platform with 96-well and 384-well plates for 3D cell culture. To generate microtissue, 50 μ L of cell suspension was seeded in each well (Fig. 24.2a, b). Spheroids were formed within 2–4 days after seeding. Long-time cell culture can finally result in cell spheroids with a dimension up to 500 μ m. The spheroids can be collected using GravityTRAP™ plate with a simple media addition step. As a product validation step, formation of micro-tissues were demonstrated with a number of cancer cell lines, including human colon (HTC-166), liver (HEP-G2), prostate (DU-145), kidney (A-498) cancer cell lines. In addition, hanging drop technique also enables cocultures of multiple cell types or spheroids by various approaches (Fig. 24.2c–e), which is useful for studying cancer invasion and cell interactions. In general, hanging drop technique provides high-throughput approach for in vitro tumor researches, especially for antitumor drug screening.

Magnetic Levitation

In the magnetic levitation method, cells or cell micro-carriers (e.g., cell encapsulating droplets or hydrogel units) are labeled with paramagnetic/diamagnetic materials and then suspended cultured in cell culture medium by balancing gravitational force with magnetic force. The levitated cells can grow in 3D space, which results in the formation of spheroids. Souza et al. demonstrated a paramagnetic cell levitation method for 3D tissue culture (Fig. 24.3a–c) [38]. Cells are first adherently cultured and incubated with hydrogels containing magnetic iron oxide nanoparticles, gold nanoparticles, and filamentous bacteriophage. The cells obtained paramagnetic property by uptaking magnetic iron oxide nanoparticles. Subsequently, the mixture of the cells and hydrogels were levitated on the liquid–air interface by applying a magnetic field through a magnet. The levitated cells and hydrogels first aggregated and then self-assembled into 3D microtissue, the shape of which is related to distribution of the magnetic field. Taking human glioblastoma cells as an example,

Table 24.1 Comparison of 3D cell culture products

| Product name | Liquid volume for each well (μL) ^a | Spheroid diameter (mm) ^b | Standard plate format (wells) | Cost (\$) ^c | Company (Website) |
|---|---|-------------------------------------|--|------------------------|--|
| GravityPLUS™ | 50 | 0.15–0.3 | 96; 384 | 140 | InSphero (http://www.insphero.com) |
| Perfecta3D® Hanging Drop Culture Plates | 25–50 | 0.1–0.4 [34, 36] | 96; 384 | 206 | 3D Biomatrix (http://3dbiomatrix.com) |
| IMAPlate™ | 25–35 | 0.05–0.3 | 96 | 33 | NCL New Concept Lab GmbH (http://www.nclnewconceptlab.com) |
| The Bio-Assembler™ System | 50–75 | 0.6–1 [38] | 1; 6 24; 96 | 600 (96-Well Kit) | Nano3D Biosciences (http://www.n3dbio.com/) |
| Rotary wall vessel | NA | Up to 10 | 55 mL 110 mL 250 mL 500 mL ^d | 5525 ^e | Synthecon, Inc. (http://www.synthecon.com) |

^aRecommended liquid volume for each well by the company. Data obtained from technical documents in corresponding websites

^bSize of spheroid after 2- to 4-day cell culture. Data obtained from technical documents in corresponding websites or published papers

^cCost for 96-well plate format

^dRotary wall vessels are sold with different volumes

^ePrice for autoclavable vessel rotary cell culture system with single station rotator base

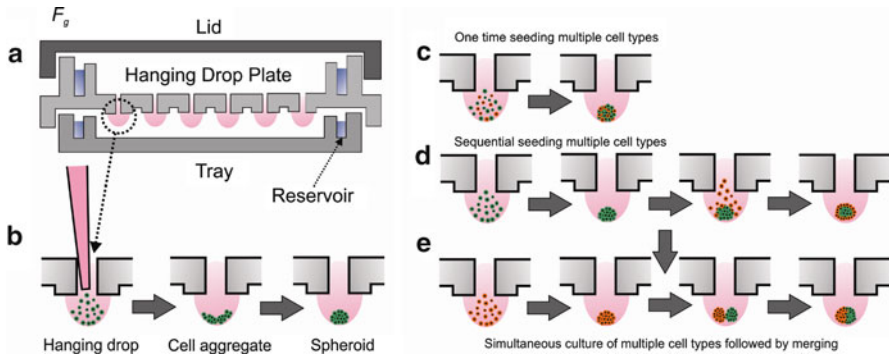


Fig. 24.2 Hanging drop technique. (a) Hanging drop plate; (b) operational procedure for hanging drop technique; (c–e) Coculture modes. (c) Simultaneous co culture multiple cell types; (d) sequential coculture multiple cell types; (e) fusion of multiple-cell-type spheroids by hanging drop technique

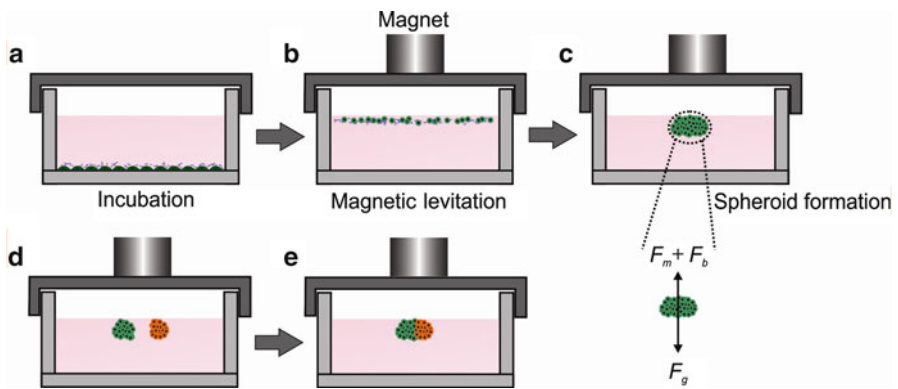


Fig. 24.3 Magnetic levitation technique. (a–c) Operational procedure for magnetic levitation technique. F_m , F_b and F_g are magnetic, buoyant and gravitational forces respectively. (d and e) Fusion of multiple-cell-type spheroids by magnetic levitation

the levitated cells self-assembled into spheroidal shape between third and eighth day and finally generated a maximum diameter of 1 mm. Morphological analysis together with molecular similarity test proved that the generated cancer spheroids were more similar to human tumor xenograft than the 2D cultured cells [38]. In addition, coculture of different cell lines was also demonstrated with human glioblastoma cells and normal astrocytes (Fig. 24.3d, e). This paramagnetic cell levitation technology has been already commercialized as a product named “The Bio-Assembler™ System” by Nano3D Biosciences (Table 24.1).

To obtain a more complex shaped microtissue, Lin et al. introduced a magnetic organoid patterning technique that allows assembly of multicellular spheroids into a complex geometry [39]. Magnetic cell spheroids were first generated using a hanging drop method by incubating cells with RGD peptide-conjugated magnetic microparticles. The spheroids were then manipulated by magnetic field and patterned into different shapes (e.g., rings, lines, and arrays). The patterned spheroids were further immobilized by thermo-responsive hydrogel and further fused together. By stacking the patterned spheroid layer by layer, complex 3D microtissues can be generated [39].

In addition, magnetic assembly of cell-encapsulating microscale hydrogels (M-gels) was developed for generation of 3D microtissues [40–42]. Both magnetic nanoparticle loaded and free radical loaded M-gels were used as building blocks for constructing various macroscopic shapes (e.g., multilayer spheroids, lines, and domes) or microscopic M-gel arrangements (e.g., square, line, and cross), respectively. Cell viability and proliferation assays indicated a good biocompatibility of this method. This method can be potentially used for modeling 3D tumor with complex structures.

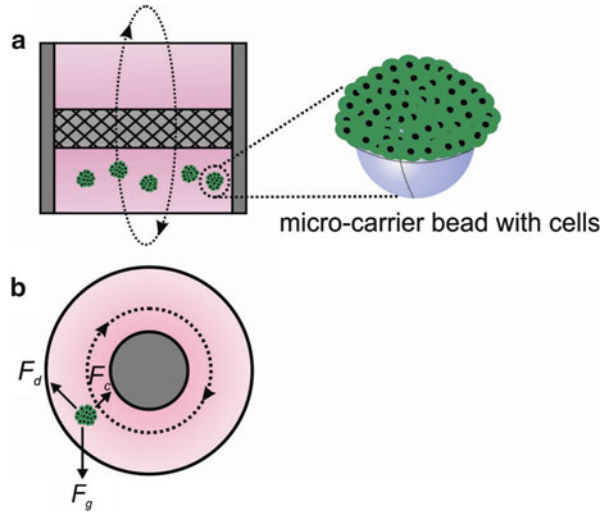
Microgravity Bioreactor

Microgravity bioreactor refers to any engineered devices or systems that enable cell or tissue culture in a very small gravity/net acceleration environment compared with that at earth surface [43–46]. Comparing with standard 2D cell culture under earth-gravitational environment, cell culture in microgravity environment possesses various advantages, including no sedimentation, loss of gravity-driven convection, decreased hydrodynamic shear and hydrostatic pressure gradient, and isotropic mass transfer based molecular diffusion. These advantages facilitate a 3D cell growth with spatially uniform cell distribution, enhanced cell-to-cell interactions, large cell harvest rate, and good cell viability.

Cell Culture in International Space Station

Cancer cells have been also cultured in microgravity environment. To obtain real microgravity environment, free fall principle is widely explored. During the free fall, gravity is supposed to be the only force acting upon an object, which results in the object losing its weight. Based on the free fall principle, a number of methods are developed to create microgravity environment with a time scale ranging from seconds to days. These methods include parabolic flight by aircraft, sub-orbital (100 km above sea level) flight by rockets, low-earth-orbit (between 160–2,000 km above sea level) flight by space shuttle and international space station (ISS). However, only low-earth-orbit space shuttle and international space station (ISS) can provide long enough duration of microgravity environment for cell culture.

Fig. 24.4 Rotating wall vessel technique. F_d , F_c and F_g are hydrodynamic drag, centripetal and gravitational forces respectively



Since 2000, a series of cancer cell culture experiments were performed in ISS to study mechanisms of tumor formation and development. For example, culture of LN1 human ovarian tumor cells and human colorectal carcinoma cells were performed in a self-contained cell incubator separately during the period of August 2001 to December 2001 in ISS Expedition 3 [47, 48]. Both cancer cell lines grew into complex 3D structures, which were much closer in true dimension and shape to original tumors found in cancer patients. These researches imply that cancer cells cultured in microgravity environment can serve as a close in vitro model to examine cancer's behavior (e.g., growth, differentiation, maturation and death) in the body, which provide an insight into seeking potential treatments for cancer and other related diseases.

Rotating Wall Vessel (One-Axis Clinostat)

Due to high cost and limited number of ISS Expedition missions, several alternative bioreactor technologies have been developed for simulation of microgravity environment on the ground. Among these technologies, rotating wall vessel (RWV) is one of widely used bioreactors originally developed by NASA [49]. RWV works as a single-axis clinostat with two concentric cylindrical surfaces (Fig. 24.4a, b). The inner surface-made is a silicone gas exchange membrane, while the outer vessel is a rotating wall that's used to generate hydrodynamic drag force. Culture medium is completely filling the space between the inner and outer cylinders. Currently, there are three different derivatives of RWV design, i.e., the slow lateral turning vessel (STLV), the high aspect ratio vessel (HARV) and the rotating wall perfused vessel (RWPV) [50, 51], out of which HARV is commercially available in the market (Table 24.1).

Both STLV and HARV have the same operational principle with a difference in their gas exchange sources. RWPV contains additional culture medium exchange column in the central cylinder for the applications in space [45, 52]. A time-averaged low gravitational field (10^{-2} to $10^{-3}g$) is created on suspended cells or cell micro-carriers in the annular space by rotating the RWV along axis perpendicular to gravitational direction at rates of 15–40 rpm. RWV has advantages, such as low shear stress (0.3 dynes cm^2), good mass transfer for nutrients and wastes exchange, which promotes the formation of large-size (5–10 mm) cancer cell spheroids. These cancer cell spheroids closely resemble the natural tumor with respect to their cellular organization and specialization. The RWV facilitates generation of 3D tumor models for various cancers, such as human breast, ovarian and prostate cancers. For example, Grun and his coworkers developed 3D cancer culture models of endometrial cancers and human ovarian cancers by RWV [53]. Both immunohistochemical profiling of multiple markers (e.g., p53, BCL2, and CA125) and proteomic profiling (e.g., prohibitin, VDAC1, and annexin 4) were performed to validate the model systems. Compared to standard 2D cancer culture models, the 3D models were more similar to the natural tumors in biological and morphological characteristics. Besides RWV, random positioning machine (RPM) is also used to simulate microgravity conditions for 3D cancer cell culture [49, 54–58]. RPM is a 3D clinostat that can rotate bioreactor along three independent axes, and it potentially offers more uniform simulated microgravity environment acting on the cells. However, three-axis clinostats are rarely used in reality due to their mechanical complexity and high cost. Some representative examples for 3D cancer culture model are given in Table 24.2. Comparison of these bioreactor technologies is also given in Table 24.3.

Bioprinting for Cancer Research

In this section, we first describe use of bioprinting technologies in developing cancer models. Then, a statistical model is described to estimate probability for single target cell encapsulation. Finally, we describe a finite-difference/front-tracking model for deposition of a compound droplet composed of cell (highly viscous droplet) and an encapsulating droplet with a flat substrate.

Bioprinting can address some of the limitations in developing 3D models such as limited repeatability, poor control over cell density, low throughput, and lack of reliable control over spatial resolution between cell types (e.g., cancer and stromal cells) in the case of coculture models [59]. Recently, a high-throughput ejector platform composed of a xyz computerized stage and two ejectors has been introduced to micropattern a 3D coculture model using cancer cells and normal fibroblasts [59] (Fig. 24.5a). In this study, OVCAR-5 and MRC-5 cells were printed within a spatially controlled microenvironment (e.g., cell density, cell–cell distance) in a high-throughput and reproducible manner. Results showed that both OVCAR-5 and MRC-5 cells remained viable during printing and sustained proliferation capacity following patterning. Such approaches can enable: (1) miniaturization of established

Table 24.2 microgravity bioreactor technologies for cancer cells

| Microgravity bioreactor | Cell type | Scaffold | Research focus | Spheroid diameter (mm) | Reference(s) |
|--------------------------|---|---|---|----------------------------------|----------------------|
| RWV | Murine melanoma cells (B16-F10) | Keratinocytes spheroids | Model of melanoma | 10 | Marrero et al. [172] |
| RWV | Glioblastoma cells (PFSK-1; KNS42; U87) | Free | Genetic, epigenetic and metabolic profiles | 9 (PFSK-1); 5 (KNS42); 1-3 (U87) | Smith et al. [173] |
| RWV | Human hepatocellular carcinoma (MHCC97H) | Poly(lactic acid-co-glycolic acid) (PLGA) | Model of human hepatocellular carcinoma in animal | 8-10 | Tang et al. [174] |
| RWV | Ovarian cancer cell (OV-TRL12B); endometrial cancer cell (EN-TRL 67T) | extracellular matrix gel from Engelbreth Holm-Swarm | Model of ovarian and endometrial cancer | 4 | Grun et al. [53] |
| RWV | Primary breast carcinomas | Free | Tumor proliferation | 1-3.5 | Becker et al. [175] |
| RWV | Murine melanoma cells (B16-F10) | Free | Melanoma growth and tumorigenicity | 5.8 | Taga et al. [176] |
| RWV | Human prostate cancer cell (LNCaP) | Type I collagen-coated dextran beads | Genetic and epigenetic profiles | 2 | Rhee et al. [177] |
| RWV | Tumor epithelial (TEC) | Free | Cell interactions | 0.5-5 | Chopra et al. [178] |
| RPM | Human malignant glioma cell (D54MG; U251MG; T98G) | Free | Tumor growth and chemosensitivity | NA | Takeda et al. [54] |
| RPM | Human follicular thyroid Carcinoma cell (ML-1) | Free | Differentiation and apoptosis | 0.3 | Grimm et al. [55] |
| MG-6C rotating clinostat | Human breast cancer cell (MCF-7) | Free | Model of breast cancer cell | NA | Qian et al. [179] |

Table 24.3 Comparison of 3D cancer cell culture technologies

| Technology | Throughput | Mass transport mechanism | Toxicity | Controllable spheroid diameter | Compatible with epifluorescence microscopy | Shear stress (dyne/cm ²) | Scaffold | Diameter | Reference(s) |
|---------------------|------------|--------------------------|--|--------------------------------|--|--------------------------------------|--|-----------|-----------------------|
| Rotating vessel | High | Laminar flow | No | No | No | ~0.8 | Collagen coated porous microbeads or scaffold free | 5–10 mm | [49, 51] |
| Magnetic levitation | Medium | Molecular diffusion | Unknown nano-toxicity and magnetic field effect on cells | Yes | Yes | 0 | Hydrogel consisting of gold, magnetic iron oxide nanoparticles and filamentous bacteriophage | 1 mm | [38] |
| Hanging drop method | High | Molecular diffusion | No | Yes | Yes | 0 | Scaffold free | 0.5 mm | [34, 36] |
| Bioprinting | High | n/a | No | Yes | Yes | Variable | Scaffold free | 10–500 μm | [59, 62, 68, 70, 142] |

macro-scale 3D culture models, (2) systematic examination into the several unidentified regulatory feedback mechanisms between stromal cells and tumor, and (3) high-throughput drug screening.

Cell encapsulation prior to bioprinting is highly probabilistic phenomena as there are several governing parameters such as number of cells that can be encapsulated, and locations of cells within a printed droplet [60, 61]. Statistical methodologies can provide an understanding of cell encapsulation process for developing 3D cancer models via bioprinting. Eventually, a reliable and repeatable control can be gained over the parameters that characterize the cell encapsulation process. Recently, a computational model of cell encapsulation process has been developed [60]. For several target cell concentrations and types of cell loading, encapsulation process was performed and captivated via a computational model (Fig. 24.5b). Probability functions, $P(X_i)$ for encapsulation of single target cells in heterogeneous cell mixture (Equation 3.6 in [60]), were plotted in Fig. 24.5c. While the percentage of target cells and homogeneity reduced in cell suspensions, each probability function, $P(X_i)$, approached a Poisson distribution (Fig. 24.5c).

Similarly, for cell printing process, computational models offer a potential to develop an understanding of how parameters, that can be adjusted experimentally, affect cell viability [62–64]. There are two critical stages during cell printing process: (1) detachment of cell encapsulating droplets from the ejector during ejection and (2) landing of cell encapsulating droplets onto receiving substrate [65, 66]. In these two stages, mechanical factors, e.g., shear stresses, hydrodynamic pressures, capillary forces, may amplify and cause deformation of droplet and cell surface. Eventually, this process may end up with cell death. However, these factors can be controlled experimentally by tuning ejection speed or by replacing encapsulating fluids with those having more suitable material properties including density, surface tension, and viscosity. Cell viability may depend on receiving surface characteristics, e.g., hydrophobicity/hydrophilicity. Prediction of cell deformation and viability via computational methods can enable researchers to successfully build 3D cancer models as well as complex viable tissue constructs [40–42, 67]. A finite-difference/front-tracking technique was described for deposition of viscous compound droplets onto a receiving surface as a model for cell printing process [68]. Inner droplet representing the cell was assumed to be a highly viscous fluid and non-wetting (not sticking to the surface) while encapsulating droplet partially wetted the substrate. A moving contact line model [69, 70] was utilized to predict the dynamic contact angle. In this study, it was also anticipated that cell viability might be correlated with deformation rate [68]. Hence, the settings that result in least cell deformation and the rate of deformation were identified. To do that, analyses were performed for a set of non-dimensional numbers, i.e., Reynolds number (Re), Weber number (We), viscosity ratio (μ_c/μ_d), surface tension ratio (σ_o/σ_i), diameter ratio (d_o/d_i), and equilibrium contact angle (θ_c). Re and We are widely used non-dimensional numbers in fluid mechanics [71] to give the ratio of inertial forces compared to viscous forces and surface tension, respectively [72, 73].

Pressure contours (left side) and pressure distribution on the surface of cell (right side) are plotted in Fig. 24.5d. Shear stresses peaked in the vicinity of the triple

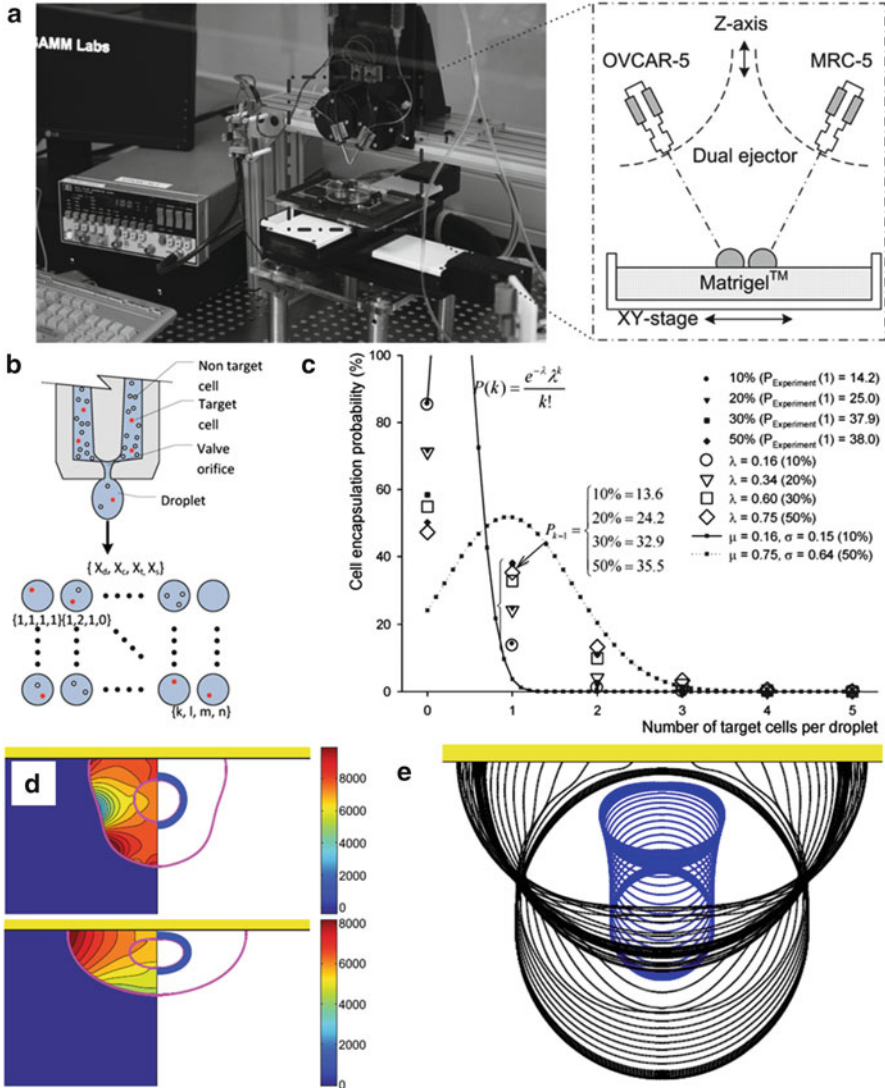


Fig. 24.5 Schematic of a high-throughput bioprinting platform composed of a *xyz* computerized stage and two ejectors diagonally aligned. Ejectors pattern cancer cells (OVCAR-5) and fibroblasts (MRC-5) simultaneously. **(b–e)** Statistical and computational modeling of cell encapsulation and printing process. **(b)** A droplet ejector was filled with heterogeneous mixture including target and non-target cells for random cell encapsulation process. (X_d) the number of droplets that contain cells, (X_c) number of cells per droplet, (X_t) number of target cells, and (X_s) droplets encapsulating a single target cell, were mapped onto a matrix of cell encapsulating droplets. **(c)** Cell encapsulation probability, $P(X)$, as a function of number of target cells per droplet for cell concentration = 1.5×10^5 cells/ml. **(d)** Pressure contours and pressure distribution on the cell were plotted at the *left half* and the *right half*, respectively. Governing non-dimensional numbers are: $We=0.5$, $Re=30$, $d_s/d_i=2.85$, $\sigma_s/\sigma_i=2541$, $\mu_s/\mu_i=10$. **(e)** Sequential impact images of cell encapsulating droplet. **(a)** is reproduced with permission [59], **(b)** and **(c)** with permission [60], and **(d)** and **(e)** with permission [68]

point during the initial phase of droplet–surface interaction. Triple point is the point where outer droplet, receiving substrate, and ambient air coincide. Maximum pressure was located near the contact line just before recoil, and migrated to the distal end from the receiving surface where it stayed there until the recoil phase. Cell geometrical deformation was defined as, $=(W_b - H_b)/(W_b + H_b)$ [68]. The computational results demonstrated that the geometrical deformation of cell monotonically increased as: (1) Re increased; (2) d_o/d_i decreased; (3) σ_o/σ_i increased; (4) μ_c/μ_d decreased; or (5) θ_c decreased. On the other hand, a local minimum, at least, of maximum geometrical deformation was obtained at $We=2$. Cell viabilities were linked to cell deformation by employing an experimental correlation of compression of cells between parallel plates [74]. Results showed that θ_c and μ_c/μ_d were highly correlated with cell viability.

To develop a better understanding of cell printing process, further computational studies have to be performed [75–78]. The described model above provided a framework to identify conditions that can increase cell viability. Next generation computational models may include non-Newtonian characteristics of flows [79–81], smaller contact angles matching better with experimental conditions, microstructured models for cells, and multiple deposition of cell encapsulating droplets.

Scaffolds (Materials/Composition Perspective)

Basement Membrane Extract

Basement membranes are sheets of ECM that form an interface between epithelial, endothelial, adipose and smooth muscle cells [82]. They contain proteins like laminin and collagen IV that play an important role in the tissue organization [82]. BD Matrigel™ and Cultrex® (Trevigine) matrixes are the examples of the reconstituted basement membrane preparations. These matrixes are extracted from a culture of Engelbreth-Holm-Swarm (EHS) mouse sarcoma. BD Matrigel™ is composed of 60 % laminin, 30 % collagen (IV), and 8 % entactin. BD Matrigel matrix also contains heparan sulfate proteoglycan (perlecan), TGF- β , EGF, insulin-like growth factor, bFGF, tissue plasminogen activator, and other growth factors along with MMP enzymes which occur naturally in the EHS tumor [82]. As these matrixes resemble the structure and composition of native basement membrane, they are extensively used for tumor cell culture studies. The SEM image of Matrigel is shown in Fig. 24.6a. Cancer cells can be mixed with liquid Matrigel which forms a 3D gel at body temperature levels. The human small cell lung carcinoma cells mixed with Matrigel were subcutaneously injected into the athymic mouse [83]. It was found that Matrigel helped tumor cells to grow whereas cells did not form large tumors when injected without Matrigel. Other cancer cell lines such as transformed mouse EHS tumor cells (T-EHS), human submandibular carcinoma A253 cells, mouse melanoma B16F10 cells, human epidermoid carcinoma KB cells, and human primary renal cell carcinoma cells were also mixed in Matrigel and coinjected subcutaneously [83]. All of these cancer cell lines rapidly formed growing tumors.

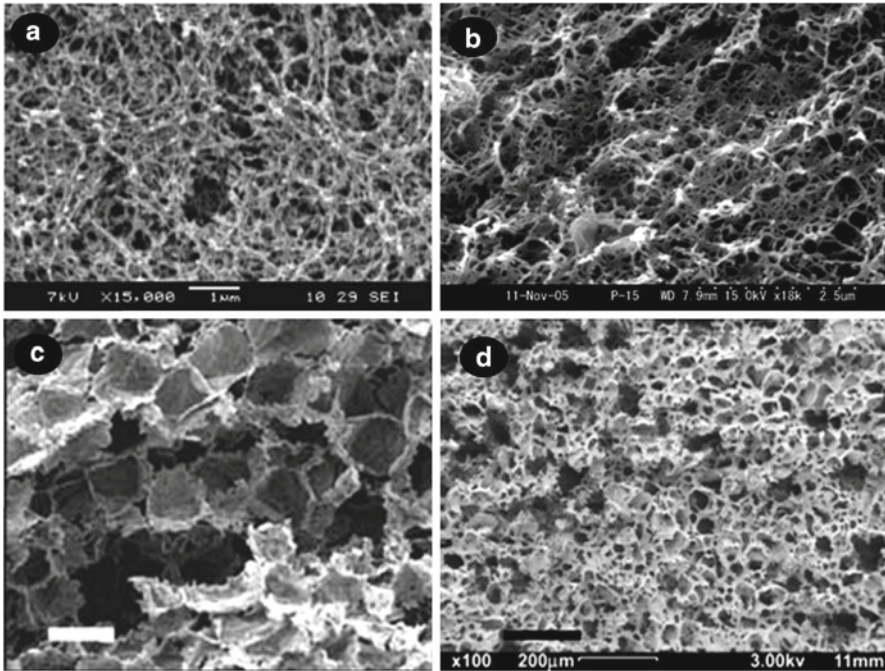


Fig. 24.6 SEM images of various scaffolds for 3D tumor models. SEM image of (a) Matrigel, (b) PuraMatrix peptide hydrogel, (c) PLG scaffold (Scale bar: 250 μm), and (d) Polystyrene scaffolds. (a) is reproduced with permission [91], (b) with permission [170], (c) with permission [109], and (d) with permission [171]

The sizes of the grown tumors, in the case of A253, KB, and B16F10 cells, were five to ten times more as compared to when cells were grown without Matrigel. These findings unequivocally describe the effects of the Matrigel in improving the growth of human tumors [83, 84]. Matrigel were also employed in coculture of preneoplastic human breast epithelial cells and breast fibroblast derived from tumor tissues [85]. The presence of fibroblast cells supported tumor invasiveness by secreting MMP enzymes which disturbed the ECM architecture. Despite these advantages, Matrigel does not fully represent tumor microenvironment as it lacks collagen (I) and hyaluronan that are present in native ECM of tumors. Collagen type I protein plays an important role in maintaining tissue architecture. Absence of these proteins from Matrigel would not guarantee the fully natural response of tumor cells.

PuraMatrix™ Peptide Hydrogel

BD™ PuraMatrix™ Peptide Hydrogel (BD™ PuraMatrix™) is a biologically inspired self-assembling peptide hydrogel (RAD16-I) matrix that is used to produce 3D microenvironments for various cell cultures including cancer cells [86].

The peptides can be self-assembled into nanofibers at physiological pH by just changing the salt concentration. The diameters of the nanofibers and interconnected pores are ~ 10 nm and 5–200 nm respectively [87, 88] as shown in Fig. 24.6b. Composition of the PuraMatrix is similar to other natural/synthetic hydrogels as it contains 99 % water and only 1 % w/v standard amino acids. The advantage of PuraMatrix is that the researchers can control the quantity of growth factors, cytokines, ECM proteins and hormones whereas Matrigel and other hydrogels contain non-quantified substances and residual growth factors [32, 89–91]. When ovarian cancer cells (OVCAR-5) were encapsulated into PuraMatrix, they assembled into 3D acinar shapes that closely resembled the shape of metastatic nodules observed clinically [86]. In another study, human hepatocellular carcinoma cells (HepG2) were mixed with PuraMatrix hydrogel and the cell mixture was hydrodynamically focused in the middle of a poly(dimethylsiloxane) channel of a microfluidic device [92]. The cells in PuraMatrix hydrogel secreted twofold more albumin than other scaffolds; quantity of albumin secretion is related to the function of liver cells [92]. New peptides can also be designed such as RADA16 and incorporated with various functional motifs including motifs derived from laminin [93], collagen [94], fibronectin [95], and bone marrow homing peptides [96]. The incorporation of these motifs enhances cell attachment, survival, and proliferation [88, 97, 98]. In one report, motifs incorporated peptide scaffolds significantly enhanced the survival and proliferation of mouse stem cells and also helped in differentiation of stem cells into neurons cells [91]. Compared to PuraMatrix, designer peptide hydrogels significantly enhanced the proliferation of mouse pre-osteoblast MC3T3-E1 cells [99].

Synthetic Scaffolds for In Vitro 3D Cancer Models

ECM structure along with various adhesion proteins and enzymes play an important role in defining tumor aggressiveness and metastatic potential. 3D scaffolds can replicate few components of natural ECM and regulate the specific cell–cell and cell–ECM interactions [2, 100]. Scaffolds have extensively been used in various tissue engineering applications including bone and cartilage [101–103]. The 3D synthetic scaffolds have interconnected microporous structures with nanotopographical features that help cells to adhere the scaffold surface and proliferate. The cell behavior is greatly dictated by physio-mechanical and chemical properties of scaffolds. Scaffolds are composed of natural molecules (Collagen, Chitosan) or synthetic polymers such as polylactide (PLA), polyglycolide (PGA), polyethylene glycol (PEG), poly(lactic-co-glycolic acid) (PLGA), and poly(lactide-co-glycolide) (PLG) [104, 105]. The stiffness of the synthetic scaffolds can be well controlled as compared to the natural scaffolds but synthetic scaffolds do not allow better cell attachment. For this purpose, either surfaces of the synthetic scaffolds need to be functionalized [106] or ECM components are premixed with scaffold solutions before synthesis [107]. In one study, PLGA and PLA polymers were used to synthesize porous microparticles using solvent evaporation method and were employed for studying 3D tumor culture [108]. Cell adhesion agents such as poly(vinyl alcohol)

and chitosan were also incorporated into the internal structure of microparticles. Different ECM components were physically adsorbed on the microparticles prior to cell seeding. The breast cancer cells (MCF-7) formed clumps on the microparticles, the morphology similar to natural tumor cells. Overall, PLA microparticles containing PVA showed better cell adhesion and growth mechanisms and gave seven times increase in cell density compared to the initial cell seeding density in 9 days [108]. PLGA and PLA are hydrophobic polymers and do not allow cell adhesion in general, but the incorporation of a hydrophilic agent such as PVA/chitosan would make scaffold's surface hydrophilic and enhances the tumor cell growth and attachment. These findings are preliminary and further clinical investigations should be done to analyze the power of microparticle based scaffold for 3D tumor modeling [108]. In another report, the PLG scaffolds were formed using the gas foaming technique and used as a 3D culture model for oral squamous cell carcinoma (OSCC-3) cells [109]. The SEM image of PLG scaffold is shown in Fig. 24.6c. Significant increase in the tumor growth was noticed when cancer cells were pre-cultured on 3D PLG scaffolds as compared to 2D culture. Angiogenic factors were also upregulated by cancer cells cultured on PLG scaffolds; 2, 23, and 98 fold increase in VEGF, bFGF, and IL-8 respectively [109]. Pre-fabricated synthetic scaffolds are also commercially available such as polystyrene scaffold (Alvetex[®] [110]) (Fig. 24.6d). These scaffolds are designed into the thin membranes so that they can fit into the conventional culture plates. The 3D porous geometry of the polystyrene scaffold facilitates cell growth, differentiation and migration [110]. It is reported that lymphoma cells (HBL-2 cells) showed increased proliferation in 3D Alvetex[®] scaffolds as compared to 2D culture plates [111]. It is evident from these reports that synthetic scaffold has great potential as 3D tumor models because their morphology and structures resemble natural ECM microenvironment. Other factors such as ECM chemical composition and proteins also influence tumor growth and aggressiveness. Synthetic scaffolds are not synthesized from natural ECM components, and therefore, getting natural response from tumor cells using synthetic scaffolds is a challenging task.

Matrix Stiffness and Fluid Flow Shear Stress for Tumor Cell Migration

Mammalian cells live in 3D microenvironments and are exposed to chemical, mechanical, and structural signals. These stimuli signals change due to disease invasion and progression through the 3D microenvironment [112–114]. Statistically nine out of ten cancer deaths is due to metastasis indicating that metastasis is the primary cause of death in cancer. Investigating the mechanical markers of single cells can help characterizing and monitoring the metastatic potential and invasiveness of cancer cells [112, 115, 116]. During metastasis, invasive cancer cells shed from the primary tumor and navigate through very tiny pores in the ECM to enter the blood vessels and circulate to create a new tumor at a remote organ [115–117]. Studying mechanical response of the invasive cancer cells to the matrix stiffness

gradient of the ECM specifically during the first stage of metastasis and intravasation can illuminate the mechanism of cancer metastasis [116]. Mak et al. explored the migration of cancer cell types in microenvironments with 3D gradients using parallel PDMS microchannels with tapered junctions that connect a large channel with a small channel. The spatially gradient tapered microchannels provide the ability to investigate the cell migration from a more confined environment to a region with greater amounts of freedom. In this case, cells were observed to migrate from wider channel to narrower channel. These results showed that MDA-MB-231 (highly metastatic) cancer cells were more invasive and therefore greater ability to migrate through the tiny high gradient microchannels where non-metastatic cancer cells (MCF-10A's) were not able to penetrate [116].

Matrix stiffness is one of the most important characteristics investigated in cellular microenvironment. Microenvironments in human body have various matrix stiffness ranging from soft such as brain with Young's modulus $E \sim 250\text{--}500$ Pa, to significantly more rigid matrixes including bone ($E \sim \text{GPa}$) and cells respond accordingly in different ECM with different mechanical stiffness. The matrix stiffness of tumors changes during the course of cancer invasion and progression [112, 118]. As an example, recent studies revealed that the breast tumor (4,000 Pa) is an order of magnitude stiffer than healthy breast tissue (200 Pa) [112]. Collagen hydrogels have been one of the most effective and widespread systems for investigating tumor cellular reaction to 3D matrixes with various stiffnesses [112, 114, 119]. This is because collagen hydrogels have physical and biochemical properties that can be altered to match the properties of tissues surrounding a tumor [119]. In a study, Casey et al. showed that the cell-scale gel microarchitecture is important in cell migration and overcome the effect of the bulk matrix density in characterizing invasive behaviors of metastatic cancer cells such as migration [119]. The tumor microenvironment matrix stiffness is a function of stromal collagen deposition and cross-linking which can alter tumor cell migration. Cancer cells employ contractile forces to change the ECM fibers surrounding tumor by aligning the fibers perpendicularly to the tumor [114, 120, 121]. Charest et al. [122] have used a 2D polyacrylamide hydrogel to develop 3D topographical features with various hydrogel stiffness. In such a system, cells are first seeded on a 2D matrix and then after spreading on the surface, cells contact the 3D features on the matrix and migrate along the 3D structures. In this investigation, cells had a higher contact length on stiffer matrixes. The traction forces produced by the cancer cells in 2D and 3D matrixes to characterize metastatic cancer cells have also been investigated [123]. These results showed that breast, lung and prostate cancer cells had metastatic ability and at the late stages of the cancer disease had significantly higher traction forces than the normal healthy tissue cells. In addition, cancer cells generated greater contractile forces on stiffer matrixes. Tumor microenvironment's mechanical properties as well as chemical properties define the degree of the traction forces [123]. Further, optical measurements and Atomic Force Microscopy (AFM) studies on the mechanical response of metastatic cancer cells have shown that these cells are more compliant compared to benign cells [123–126]. The metastatic cancer cells are then more plastic and therefore are able to easily migrate through the ECM [123].

During the first stage of metastasis, the ECM around the tumor degrades due to the action of matrix MMPs [127–129]. Fluid shear stress is one of the extracellular stimuli that modulate MMP genes [130], and therefore, shear forces could potentially alter the migratory response of cancer cells. Qazi et al. investigated shear stress as a main controller of cell migration that helped explaining the differences between the invasiveness glioma cells in vitro compared to in vivo [129]. This work explains the diverse migratory response of tumor cells and differential invasiveness of the cancer cells due to fluid flow forces and shear stress. These results show that the motility of glioma cells can be reduced due to the shear stress by changing the MMP expression [129]. Recently, the role of fluidic shear stress on the metastatic potential of epithelial ovarian cancer cells was investigated using microfluidic platform. The ovarian cancer cells showed enhanced epithelial–mesenchymal transition and metastatic potential only when cultured under continuous and controlled laminar flow [131].

Conclusions and Future Perspectives

Tumor tissues and carcinomas are comprised of a 3D spatially organized ECM [38, 132–135] with multiple cell types [136, 137]. For in vitro cancer models, presence of multiple cell types is critical as the stromal cells play a critical role in malignant progression of tumor including angiogenesis [136], metastasis [138], and invasiveness [139], and these cell types are important targets for tumor therapies [140]. Presence and spatial positioning of neighboring cells are important factors when studying the precise role of stromal cells in tumors [141, 142]. There are several technologies that can precisely position different cell types in a 3D setting, such as bioprinting [41, 42, 143–146], microfabrication [147], and microscale assembly [40–42, 148]. These methods can potentially be used to create 3D cancer models and to study the interaction between different cell types [149]. In embedded and overlay cultures, basement membranes can promote 3D cellular organizations by establishing biologically relevant contact between cells and substratum [30]. Culturing cells in 3D suspension is another way of creating 3D cell cultures by reducing the adhesion between cells and the substratum. Hanging drop is a promising method to create 3D cell culture models through aggregation of cells at a spherical air–liquid interface within hanging drops [34–37]. Cells can be magnetically labeled with paramagnetic/diamagnetic materials and suspended in culture medium using magnetic levitation and gravitational force to create 3D tissue cultures [38]. Microscale hydrogels encapsulating cells have also been assembled using magnetic assembly that can be used potentially for 3D cancer models [40–42]. Bioprinting technology is a repeatable, reliable, and high-throughput method that utilizes a programmable and automated stage with ejectors to bioprint different cell types and to create 3D coculture cancer models [59, 150]. Controlling cell culture in low gravitational forces is another way of facilitating 3D cell growth in a spatially uniform cell distribution [43–46]. Microgravity bioreactor [43–46], rotating wall vessel [49], and cell culture in international space [47, 48] are three examples of such methods as these techniques were discussed in detail in this chapter.

Cells cultured as 2D monolayers showed substantial mutations in gene expression compared to cells in 3D cultures and native tissues [151, 152]. Cancer cells cultured on 2D versus 3D microenvironments display dissimilar cell morphology [153], metabolic characteristics, and drug response [154]. Moreover, genes responsible for angiogenesis, chemokine generation, cell migration and adhesion have different expression levels between 2D and 3D settings [155, 156]. Importantly, cancer cells are known to display different behavior to chemotherapeutic drugs in 3D culture compared to 2D controls [157]. Cumulative evidence in the literature demonstrates that *in vitro* 3D cancer models better recapitulate *in vivo* conditions and response compared to 2D cultures [153, 158, 159]. There are also cancer types (e.g., Ewing's sarcoma) for which the currently available murine models and murine cells perform poorly compared to *in vitro* models employing human cells [160]. For these cancer types, human cells need to be used in 3D culture conditions to effectively represent the *in vivo* conditions.

There are many factors that need to be considered in a 3D *in vitro* cancer models to produce a characteristic feature of the *in vivo* 3D solid tumors. In embedded and overlay cell culture, 3D models provide the space for cell migration and proliferation, which mimic the 3D *in vivo* models [31]. RWV cancer models also provide a 3D microenvironment that were validated to produce a characteristic feature of the tumor by immunohistochemical profiling of multiple markers such as p53, BCL2, and CA125 and proteomic profiling such as prohibitin, VDAC1, and annexin 4 [53]. Multicellular spheroids mimic the native tumor microenvironment and emulate the drug-resistant hypoxia regions at the center of grown tumor mass [161]. On the other hand, these spheroids do not emulate the *in vivo* blood vessel barrier due to direct contact with culture media of cancer cells in spheroids [162, 163]. The spheroid culture do not fully provide *in vivo* host immune interactions during tumor growth [161]. In basement membrane tumor models, such as BD Matrigel matrix, the effect of multiple parameters that occur in a solid tumor including heparan sulfate proteoglycan (perlecan), TGF- β , EGF, insulin-like growth factor, bFG, tissue plasminogen activator, and MMP enzymes have been considered. However, Matrigel 3D cancer model lacks collagen-1 and hyaluronan that are essential in maintaining the architecture of tissue. The absence of these proteins affect the cancer cell response in a 3D model [82]. It was reported that mammary epithelial cells self-assembled into spherical structures with a central lumen resembling natural mammary acini, when cultured on laminin-rich basement membrane [164]. In another report, the epithelial cells have inverse polarity and did not form central lumen when cultured on 3D collagen gels alone, whereas they showed normal polarity and central lumen structure when cocultured with myoepithelial cells. The myoepithelial cells deposited the basement membrane component laminin-1 which was an important factor to determine the tumor polarity and central lumen formation. [165]. It clearly points out that ECM components have a significant effect on morphology and polarity of cancer cells during tumor cancer growth. Bioprinting is a high-throughput technology that can produce 3D cancer models repeatably with a reliable control over spatial resolution. In one report, ovarian cancer cells (OVCAR-5) and fibroblast cells (MRC-5)

were patterned on Matrigel using a bioprinting platform. The cancer cells spontaneously formed multicellular acini structures that resembled the polarity of the tumor [59]. The coculture of cancer and supporting stromal cells at various cell densities were overlaid successfully using the bioprinting technique [59]. However, more studies have to be conducted to show if such a platform mimics the aggressive and invasive characteristics of tumor cells.

In order to minimize the animal testing and cost, there is a need for 3D in vitro tissue models, which are scalable, can be produced with high-throughput methods and that mimic the tissue native microenvironment [166]. Scaffold-free 3D micro-tissue models are considered more organotypic and compatible with high-throughput technologies. They are currently being developed and used with automated production platform for tumor microtissues [167]. High-throughput bioscreening allows systematic and quantitative screening of chemotherapeutic drugs, supporting rapid pharmacokinetic and pharmacodynamic analyses. Since throughput is critical in cancer research, where large compound libraries are evaluated regularly with many different cell types, advanced assembly/fabrication technologies with precise compositional and spatial control over cells to establish 3D platforms are needed [149, 168]. Automation and miniaturization of these technologies would also allow rapid and effective fabrication of a large scale of 3D in vitro tissue models with patient's own cells, which then can be used to screen a palette of therapeutic candidates and to match the best fit with the patient in a personalized manner. Future 3D models of complex tissues and tumors also need to take into consideration the physiological environment, such as the mechanical microenvironment including fluid flow and mechanical forces in play.

References

1. Globocan 2008 (2010) International Agency for Research on Cancer (IARC), World Health Organization. <http://globocan.iarc.fr/factsheets/populations/factsheet.asp?uno=900>
2. Bissell MJ, Radisky D (2001) Putting tumours in context. *Nat Rev Cancer* 1(1):46
3. Hanahan D, Weinberg RA (2000) The hallmarks of cancer. *Cell* 100(1):57–70
4. Alberts B, Johnson A, Lewis J, Raff M, Roberts K, Walter P (2002) *Molecular biology of the cell*, 4th edn. Garland Science, New York
5. Johansson N, Ahonen M, Kahari VM (2000) Matrix metalloproteinases in tumor invasion. *Cell Mol Life Sci* 57(1):5–15
6. Calmels TPG, Mattot V, Wernert N, Vandebunder B, Stehelin D (1995) Invasive tumors induce c-ets1 transcription factor expression in adjacent stroma. *Biol Cell* 84(1–2):53–61
7. Kerbel R, Folkman J (2002) Clinical translation of angiogenesis inhibitors. *Nat Rev Cancer* 2(10):727–739
8. Hortobagyi GN (2004) Opportunities and challenges in the development of targeted therapies. In: *Seminars in oncology*. Elsevier, 31(3):21–27
9. Abbott A (2003) Cell culture: biology's new dimension. *Nature* 424(6951):870–872
10. Wang F, Weaver VM, Petersen OW, Larabell CA, Dedhar S, Briand P, Lupu R, Bissell MJ (1998) Reciprocal interactions between beta1-integrin and epidermal growth factor receptor in three-dimensional basement membrane breast cultures: a different perspective in epithelial biology. *Proc Natl Acad Sci* 95(25):14821–14826

11. Liu H, Radisky DC, Wang F, Bissell MJ (2004) Polarity and proliferation are controlled by distinct signaling pathways downstream of pi3-kinase in breast epithelial tumor cells. *J Cell Biol* 164(4):603–612
12. Weaver VM, Lelievre S, Lakin JN, Chrenek MA, Jones JCR, Giancotti F, Werb Z, Bissell MJ (2002) Beta4 integrin-dependent formation of polarized three-dimensional architecture confers resistance to apoptosis in normal and malignant mammary epithelium. *Cancer Cell* 2(3):205–216
13. Durand RE, Olive PL (2001) Resistance of tumor cells to chemo- and radiotherapy modulated by the three-dimensional architecture of solid tumors and spheroids. *Methods Cell Biol* 64:211–233
14. Kerbel RS (1994) Impact of multicellular resistance on the survival of solid tumors, including micrometastases. *Invasion Metastasis* 14(1–6):50
15. Hauptmann S, Denkert C, Lohrke H, Tietze L, Ott S, Klosterhalfen B, Mittermayer C (1995) Integrin expression on colorectal tumor cells growing as monolayers, as multicellular tumor spheroids, or in nude mice. *Int J Cancer* 61(6):819–825
16. Voskoglou-Nomikos T, Pater JL, Seymour L (2003) Clinical predictive value of the in vitro cell line, human xenograft, and mouse allograft preclinical cancer models. *Clin Cancer Res* 9(11):4227–4239
17. Richmond A, Su Y (2008) Mouse xenograft models vs gem models for human cancer therapeutics. *Dis Model Mech* 1(2–3):78–82
18. Becher OJ, Holland EC (2006) Genetically engineered models have advantages over xenografts for preclinical studies. *Cancer Res* 66(7):3355–3359
19. Olive KP, Tuveson DA (2006) The use of targeted mouse models for preclinical testing of novel cancer therapeutics. *Clin Cancer Res* 12(18):5277–5287
20. Frese KK, Tuveson DA (2007) Maximizing mouse cancer models. *Nat Rev Cancer* 7(9):654–658
21. Loudos G, Kagadis GC, Psimadas D (2011) Current status and future perspectives of in vivo small animal imaging using radiolabeled nanoparticles. *Eur J Radiol* 78(2):287–295
22. Hahn MA, Singh AK, Sharma P, Brown SC, Moudgil BM (2011) Nanoparticles as contrast agents for in-vivo bioimaging: current status and future perspectives. *Anal Bioanal Chem* 399(1):3–27
23. Kagadis GC, Loudos G, Katsanos K, Langer SG, Nikiforidis GC (2010) In vivo small animal imaging: current status and future prospects. *Med Phys* 37:6421
24. Cai W, Chen X (2008) Multimodality molecular imaging of tumor angiogenesis. *J Nucl Med* 49(Suppl 2):113S–128S
25. Boehm T, Folkman J, Browder T, O'Reilly MS (1997) Antiangiogenic therapy of experimental cancer does not induce acquired drug resistance. *Nature* 390(6658):404–407
26. Browder T, Butterfield CE, Kraling BM, Shi B, Marshall B, O'Reilly MS, Folkman J (2000) Antiangiogenic scheduling of chemotherapy improves efficacy against experimental drug-resistant cancer. *Cancer Res* 60(7):1878–1886
27. Eder JP Jr, Supko JG, Clark JW, Puchalski TA, Garcia-Carbonero R, Ryan DP, Shulman LN, Proper J, Kirvan M, Rattner B (2002) Phase I clinical trial of recombinant human endostatin administered as a short intravenous infusion repeated daily. *J Clin Oncol* 20(18):3772–3784
28. Breslin S, O'Driscoll L (2013) Three-dimensional cell culture: the missing link in drug discovery. *Drug Discov Today* 18(5–6):240–249
29. Soares CP, Midlej V, Oliveira M, Benchimol M, Costa ML, Mermelstein C (2012) 2d and 3d-organized cardiac cells shows differences in cellular morphology, adhesion junctions, presence of myofibrils and protein expression. *PLoS One* 7(5):e38147
30. Zhou S, Li F, Xiao J, Xiong W, Fang Z, Chen W, Niu P (2010) Isolation and identification of cancer stem cells from human osteosarcoma by serum-free three-dimensional culture combined with anticancer drugs. *J Huazhong Univ Sci Technolog Med Sci* 30(1):81–84
31. Linde N, Gutschalk CM, Hoffmann C, Yilmaz D, Mueller MM (2012) Integrating macrophages into organotypic co-cultures: a 3d in vitro model to study tumor-associated macrophages. *PLoS One* 7(7):e40058

32. Kleinman HK, McGarvey ML, Hassell JR, Star VL, Cannon FB, Laurie GW, Martin GR (1986) Basement membrane complexes with biological activity. *Biochemistry* 25(2):312–318
33. Wang AZ, Ojakian GK, Nelson WJ (1990) Steps in the morphogenesis of a polarized epithelium. *J Cell Sci* 95:137–151
34. Hsiao AY, Tung Y-C, Qu X, Patel LR, Pienta KJ, Takayama S (2012) 384 hanging drop arrays give excellent z-factors and allow versatile formation of co-culture spheroids. *Biotechnol Bioeng* 109(5):1293–1304
35. Hsiao AY, Tung YC, Kuo CH, Mosadegh B, Bedenis R, Pienta KJ, Takayama S (2012) Micro-ring structures stabilize microdroplets to enable long term spheroid culture in 384 hanging drop array plates. *Biomed Microdevices* 14(2):313–323
36. Tung Y-C, Hsiao AY, Allen SG, Y-s T, Ho M, Takayama S (2011) High-throughput 3d spheroid culture and drug testing using a 384 hanging drop array. *Analyst* 136(3):473–478
37. Lee WG, Ortmann D, Hancock MJ, Bae H, Khademhosseini A (2010) A hollow sphere soft lithography approach for long-term hanging drop methods. *Tissue Eng Part C Methods* 16(2):249–259
38. Souza GR, Molina JR, Raphael RM, Ozawa MG, Stark DJ, Levin CS, Bronk LF, Ananta JS, Mandelin J, Georgescu M-M, Bankson JA, Gelovani JG, Killian TC, Arap W, Pasqualini R (2010) Three-dimensional tissue culture based on magnetic cell levitation. *Nat Nanotechnol* 5(4):291–296
39. Lin R-Z, Chu W-C, Chiang C-C, Lai C-H, Chang H-Y (2008) Magnetic reconstruction of three-dimensional tissues from multicellular spheroids. *Tissue Eng Part C Methods* 14(3):197–205
40. Tasoglu S, Kavaz D, Gurkan UA, Guven S, Chen P, Zheng R, Demirci U (2013) Paramagnetic levitational assembly of hydrogels. *Adv Mater* 25(8):1137–1143
41. Xu F, Finley TD, Turkeydin M, Sung Y, Gurkan UA, Yavuz AS, Guldiken RO, Demirci U (2011) The assembly of cell-encapsulating microscale hydrogels using acoustic waves. *Biomaterials* 32(31):7847–7855
42. Xu F, Wu CAM, Rengarajan V, Finley TD, Keles HO, Sung YR, Li BQ, Gurkan UA, Demirci U (2011) Three-dimensional magnetic assembly of microscale hydrogels. *Adv Mater* 23(37):4254–4260
43. Barzegari A, Saei AA (2012) An update to space biomedical research: tissue engineering in microgravity bioreactors. *BioImpacts* 2(1):23–32
44. Maxson S, Orr D, Burg KJL (2011) Bioreactors for tissue engineering. *Tissue engineering: from lab to clinic*. Springer, Berlin
45. Chen HC, Hu YC (2006) Bioreactors for tissue engineering. *Biotechnol Lett* 28(18):1415–1423
46. Martin I, Wendt D, Heberer M (2004) The role of bioreactors in tissue engineering. *Trends Biotechnol* 22(2):80–86
47. Becker JL (2013) Cellular biotechnology operations support systems: evaluation of ovarian tumor cell growth and gene expression (cboss-01-ovarian). http://www.nasa.gov/mission_pages/station/research/experiments/248.html
48. Jessup JM (2013) Cellular biotechnology operations support systems: use of NASA bioreactor to study cell cycle regulation: mechanisms of colon carcinoma metastasis in microgravity. http://www.nasa.gov/mission_pages/station/research/experiments/CBOSS-01-Colon.html
49. Navran S (2008) The application of low shear modeled microgravity to 3-d cell biology and tissue engineering. In: El-Gewely MR (ed) *Biotechnology annual review*, vol 14. Elsevier, Amsterdam, pp 275–296
50. Begley CM, Kleis SJ (2002) Rwpv bioreactor mass transport: earth-based and in microgravity. *Biotechnol Bioeng* 80(4):465–476
51. Barrila J, Radtke AL, Crabbé A, Sarker SF, Herbst-Kralovetz MM, Ott CM, Nickerson CA (2010) Organotypic 3d cell culture models: Using the rotating wall vessel to study host-pathogen interactions. *Nat Rev Microbiol* 8(11):791–801
52. Freed LE, Langer R, Martin I, Pellis NR, Vunjak-Novakovic G (1997) Tissue engineering of cartilage in space. *Proc Natl Acad Sci* 94(25):13885–13890

53. Grun B, Benjamin E, Sinclair J, Timms JF, Jacobs JJ, Gayther SA, Dafou D (2009) Three-dimensional in vitro cell biology models of ovarian and endometrial cancer. *Cell Prolif* 42(2):219–228
54. Takeda M, Magaki T, Okazaki T, Kawahara Y, Manabe T, Yuge L, Kurisu K (2009) Effects of simulated microgravity on proliferation and chemosensitivity in malignant glioma cells. *Neurosci Lett* 463(1):54–59
55. Grimm D, Bauer J, Kossmehl P, Shakibaei M, Schonberger J, Pickenhahn H, Schulze-Tanzil G, Vetter R, Eilles C, Paul M, Cogoli A (2002) Simulated microgravity alters differentiation and increases apoptosis in human follicular thyroid carcinoma cells. *FASEB J* 16(2):604–606
56. Han ZB, Ishizaki K, Nishizawa K, Kato T, Todo T, Ikenaga M (1999) A genetic effect of altered gravity: Mutations induced by simulated hypogravity and hypergravity in microsatellite sequences of human tumor cells. *Mutat Res* 426(1):1–10
57. Hammer BE, Kidder LS, Williams PC, Xu WW (2009) Magnetic levitation of mc3t3 osteoblast cells as a ground-based simulation of microgravity. *Microgravity Sci Technol* 21(4):311–318
58. Nishikawa M, Ohgushi H, Tamai N, Osuga K, Uemura M, Yoshikawa H, Myoui A (2005) The effect of simulated microgravity by three-dimensional clinostat on bone tissue engineering. *Cell Transplant* 14(10):829–835
59. Xu F, Celli J, Rizvi I, Moon S, Hasan T, Demirci U (2011) A three-dimensional in vitro ovarian cancer coculture model using a high-throughput cell patterning platform. *Biotechnol J* 6(2):204–212
60. Moon S, Ceyhan E, Gurkan UA, Demirci U (2011) Statistical modeling of single target cell encapsulation. *PLoS One* 6(7):e21580
61. Ceyhan E, Xu F, Gurkan UA, Emre AE, Turali ES, El Assal R, Acikgenc A, Wu CM, Demirci U (2012) Prediction and control of number of cells in microdroplets by stochastic modeling. *Lab on a Chip*. doi:[10.1039/C1032LC40523G](https://doi.org/10.1039/C1032LC40523G)
62. Tasoglu S, Demirci U (2013) Bioprinting for stem cell research. *Trends Biotechnol* 31(1):10–19
63. Demirci U, Khademhosseini A, Langer R, Blander J (2012) *Microfluidic technologies for human health*. World Scientific Publishing Company, Singapore
64. Tasoglu S, Gurkan UA, Wang A, Demirci U (2013) Manipulating biological agents and cells in microscale volumes for applications in medicine. *Chem Soc Rev* 13(42):5788–5808
65. Demirci U, Montesano G (2007) Cell encapsulating droplet vitrification. *Lab Chip* 7(11):1428–1433
66. Demirci U, Montesano G (2007) Single cell epitaxy by acoustic picoliter droplets. *Lab Chip* 7:1139–1145
67. Gurkan UA, Tasoglu S, Kavaz D, Demirel MC, Demirci U (2012) Emerging technologies for assembly of microscale hydrogels. *Adv Healthc Mater* 1(2):149–158
68. Tasoglu S, Kaynak G, Szeri AJ, Demirci U, Muradoglu M (2010) Impact of a compound droplet on a flat surface: a model for single cell epitaxy. *Phys Fluids* 22(8)
69. Kistler SF (ed) (1993) *Wettability*. Dekker, New York
70. Muradoglu M, Tasoglu S (2010) A front-tracking method for computational modeling of impact and spreading of viscous droplets on solid walls. *Comput Fluids* 39(4):615–625
71. Tasoglu S, Rohan LC, Katz DF, Szeri AJ (2013) Transient swelling, spreading and drug delivery by a dissolved anti-hiv microbicide-bearing film. *Phys Fluids* 25(3):031901–031916 (<http://dx.doi.org/10.1063/1.4793598>)
72. Szeri AJ, Park SC, Tasoglu S, Verguet S, Gorham A, Gao Y, Katz DF (2010) Epithelial coating mechanisms by semi-solid materials: application to microbicide gels. *Biophys J* 98(3):604
73. Tasoglu S, Peters JJ, Park SC, Verguet S, Katz DF, Szeri AJ (2011) The effects of inhomogeneous boundary dilution on the coating flow of an anti-HIV microbicide vehicle. *Phys Fluids* 23(9):093101
74. Takamatsu H, Rubinsky B (1999) Viability of deformed cells. *Cryobiology* 39(3):243–251

75. Moon S, Hasan SK, Song YS, Xu F, Keles HO, Manzur F, Mikkilineni S, Hong JW, Nagatomi J, Haeggstrom E, Khademhosseini A, Demirci U (2010) Layer by layer three-dimensional tissue epitaxy by cell-laden hydrogel droplets. *Tissue Eng Part C Methods* 16(1):157–166
76. Xu F, Moon SJ, Emre AE, Turali ES, Song YS, Hacking SA, Nagatomi J, Demirci U (2010) A droplet-based building block approach for bladder smooth muscle cell (smc) proliferation. *Biofabrication* 2(1):9
77. Moon S, Kim YG, Dong L, Lombardi M, Haeggstrom E, Jensen RV, Hsiao LL, Demirci U (2011) Drop-on-demand single cell isolation and total RNA analysis. *PLoS One* 6(3):e17455
78. Samot J, Moon S, Shao L, Zhang X, Xu F, Song Y, Keles HO, Matloff L, Markel J, Demirci U (2011) Blood banking in living droplets. *PLoS One* 6(3):e17530
79. Tasoglu S, Park SC, Peters JJ, Katz DF, Szeri AJ (2011) The consequences of yield stress on deployment of a non-newtonian anti-HIV microbicide gel. *J Nonnewton Fluid Mech* 166(19–20):1116–1122
80. Tasoglu S, Katz DF, Szeri AJ (2012) Transient spreading and swelling behavior of a gel deploying an anti-HIV microbicide. *Journal of Non-Newtonian Fluid Mechanics* 187:36–42
81. Tasoglu S, Szeri AJ, Katz DF (2011) Transport processes in vaginal films that release anti-HIV microbicide molecules. *Biophys J* 100(3):489
82. Kleinman HK, Martin GR (2005) Matrigel: Basement membrane matrix with biological activity. In: *Seminars in cancer biology*. Elsevier, 15(5):378–386
83. Fridman R, Kibbey MC, Royce LS, Zain M, Sweeney TM, Jicha DL, Yannelli JR, Martin GR, Kleinman HK (1991) Enhanced tumor growth of both primary and established human and murine tumor cells in athymic mice after coinjection with matrigel. *J Natl Cancer Inst* 83(11):769–774
84. Webber MM, Bello D, Kleinman HK, Hoffman MP (1997) Acinar differentiation by non-malignant immortalized human prostatic epithelial cells and its loss by malignant cells. *Carcinogenesis* 18(6):1225–1231
85. Shekhar MPV, Werdell J, Santner SJ, Pauley RJ, Tait L (2001) Breast stroma plays a dominant regulatory role in breast epithelial growth and differentiation: Implications for tumor development and progression. *Cancer Res* 61(4):1320–1326
86. Adnan OA-Y, Imran R, Conor LE, Jonathan PC, Tayyaba H (2009) Puramatrix encapsulation of cancer cells. *J Vis Exp* (34)
87. Zhang S, Holmes T, Lockshin C, Rich A (1993) Spontaneous assembly of a self-complementary oligopeptide to form a stable macroscopic membrane. *Proc Natl Acad Sci* 90(8):3334–3338
88. Zhang S, Holmes TC, DiPersio CM, Hynes RO, Su X, Rich A (1995) Self-complementary oligopeptide matrices support mammalian cell attachment. *Biomaterials* 16(18):1385–1393
89. Weaver VM, Howlett AR, Langton-Webster B, Petersen OW, Bissell MJ (1995) The development of a functionally relevant cell culture model of progressive human breast cancer. In: *Seminars in cancer biology*. Elsevier, 6(3):175–184
90. Spancake KM, Anderson CB, Weaver VM, Matsunami N, Bissell MJ, White RL (1999) E7-transduced human breast epithelial cells show partial differentiation in three-dimensional culture. *Cancer Res* 59(24):6042–6045
91. Gelain F, Bottai D, Vescovi A, Zhang S (2006) Designer self-assembling peptide nanofiber scaffolds for adult mouse neural stem cell 3-dimensional cultures. *PLoS One* 1(1):e119
92. Kim MS, Yeon JH, Park J-K (2007) A microfluidic platform for 3-dimensional cell culture and cell-based assays. *Biomed Microdevices* 9(1):25–34
93. Ranieri JP, Bellamkonda R, Bekos EJ, Vargo TG, Gardella JA, Aebischer P (2004) Neuronal cell attachment to fluorinated ethylene propylene films with covalently immobilized laminin oligopeptides YIGSR and IKVAV. II. *J Biomed Mater Res* 29(6):779–785
94. Knight CG, Morton LF, Peachey AR, Tuckwell DS, Farndale RW, Barnes MJ (2000) The collagen-binding α -domains of integrins $\alpha(1)\beta(1)$ and $\alpha(2)\beta(1)$ recognize the same specific amino acid sequence, GFOGER, in native (triple-helical) collagens. *J Biol Chem* 275(1):35–40

95. Ruoslahti E, Pierschbacher MD (1987) New perspectives in cell adhesion: RGD and integrins. *Science* 238(4826):491
96. Nowakowski GS, Dooner MS, Valinski HM, Mihaliak AM, Quesenberry PJ, Becker PS (2004) A specific heptapeptide from a phage display peptide library homes to bone marrow and binds to primitive hematopoietic stem cells. *Stem Cells* 22(6):1030–1038
97. Kisiday J, Jin M, Kurz B, Hung H, Semino C, Zhang S, Grodzinsky AJ (2002) Self-assembling peptide hydrogel fosters chondrocyte extracellular matrix production and cell division: implications for cartilage tissue repair. *Proc Natl Acad Sci* 99(15):9996–10001
98. Davis ME, Motion JPM, Narmoneva DA, Takahashi T, Hakuno D, Kamm RD, Zhang S, Lee RT (2005) Injectable self-assembling peptide nanofibers create intramyocardial microenvironments for endothelial cells. *Circulation* 111(4):442–450
99. Horii A, Wang X, Gelain F, Zhang S (2007) Biological designer self-assembling peptide nanofiber scaffolds significantly enhance osteoblast proliferation, differentiation and 3-d migration. *PLoS One* 2(2):e190
100. Barcellos-Hoff MH, Medina D (2005) New highlights on stroma-epithelial interactions in breast cancer. *Breast Cancer Res* 7(1):33–36
101. Karp JM, Dalton PD, Shoichet MS (2003) Scaffolds for tissue engineering. *MRS Bull* 28(4):301–306
102. Asghar W, Kim YT, Ilyas A, Sankaran J, Wan Y, Iqbal SM (2012) Synthesis of nano-textured biocompatible scaffolds from chicken eggshells. *Nanotechnology* 23(47):475601–475609
103. Huttmacher DW (2000) Scaffolds in tissue engineering bone and cartilage. *Biomaterials* 21(24):2529–2543
104. Buurma B, Gu K, Rutherford RB (2003) Transplantation of human pulpal and gingival fibroblasts attached to synthetic scaffolds. *Eur J Oral Sci* 107(4):282–289
105. Asghar W, Islam M, Wadajkar AS, Wan Y, Ilyas A, Nguyen KT, Iqbal SM (2012) PLGA micro- and nanoparticles loaded into gelatin scaffold for controlled drug release. *IEEE T Nanotech* 11(3):546–553
106. Cunliffe D, Pennadam S, Alexander C (2004) Synthetic and biological polymers-merging the interface. *Eur Polym J* 40(1):5–25
107. Chen G, Sato T, Ushida T, Hirochika R, Shirasaki Y, Ochiai N, Tateishi T (2003) The use of a novel PLGA fiber/collagen composite web as a scaffold for engineering of articular cartilage tissue with adjustable thickness. *J Biomed Mater Res A* 67(4):1170–1180
108. Sahoo SK, Panda AK, Labhasetwar V (2005) Characterization of porous PLGA/PLA microparticles as a scaffold for three dimensional growth of breast cancer cells. *Biomacromolecules* 6(2):1132–1139
109. Fischbach C, Chen R, Matsumoto T, Schmelzle T, Brugge JS, Polverini PJ, Mooney DJ (2007) Engineering tumors with 3d scaffolds. *Nat Methods* 4(10):855–860
110. Knight E, Murray B, Carnachan R, Przyborski S (2011) Alvetex®: polystyrene scaffold technology for routine three dimensional cell culture. *Methods Mol Biol* 695:323–340
111. Caicedo-Carvajal CE, Liu Q, Remache Y, Goy A, Suh KS (2011) Cancer tissue engineering: a novel 3d polystyrene scaffold for in vitro isolation and amplification of lymphoma cancer cells from heterogeneous cell mixtures. *J Tissue Eng* 2(1)
112. Paszek MJ, Zahir N, Johnson KR, Lakins JN, Rozenberg GI, Gefen A, Reinhart-King CA, Margulies SS, Dembo M, Boettiger D, Hammer DA, Weaver VM (2005) Tensional homeostasis and the malignant phenotype. *Cancer Cell* 8(3):241–254
113. Conklin MW, Eickhoff JC, Riching KM, Pehlke CA, Eliceiri KW, Provenzano PP, Friedl A, Keely PJ (2011) Aligned collagen is a prognostic signature for survival in human breast carcinoma. *Am J Pathol* 178(3):1221–1232
114. Kraning-Rush CM, Reinhart-King CA (2012) Controlling matrix stiffness and topography for the study of tumor cell migration. *Cell Adh Migr* 6(3):274–279
115. Chambers AF, Groom AC, MacDonald IC (2002) Dissemination and growth of cancer cells in metastatic sites. *Nat Rev Cancer* 2(8):563–572
116. Mak M, Reinhart-King CA, Erickson D (2011) Microfabricated physical spatial gradients for investigating cell migration and invasion dynamics. *PLoS One* 6(6):e20825
117. Sahai E (2007) Illuminating the metastatic process. *Nat Rev Cancer* 7(10):737–749

118. Levental KR, Yu H, Kass L, Lakins JN, Egeblad M, Erler JT, Fong SF, Csiszar K, Giaccia A, Wenginger W, Yamauchi M, Gasser DL, Weaver VM (2009) Matrix crosslinking forces tumor progression by enhancing integrin signaling. *Cell* 139(5):891–906
119. Carey SP, Kraning-Rush CM, Williams RM, Reinhart-King CA (2012) Biophysical control of invasive tumor cell behavior by extracellular matrix microarchitecture. *Biomaterials* 33(16):4157–4165
120. Provenzano PP, Inman DR, Eliceiri KW, Trier SM, Keely PJ (2008) Contact guidance mediated three-dimensional cell migration is regulated by Rho/ROCK-dependent matrix reorganization. *Biophys J* 95(11):5374–5384
121. Provenzano PP, Eliceiri KW, Campbell JM, Inman DR, White JG, Keely PJ (2006) Collagen reorganization at the tumor-stromal interface facilitates local invasion. *BMC Med* 4(1):38
122. Charest JM, Califano JP, Carey SP, Reinhart-King CA (2012) Fabrication of substrates with defined mechanical properties and topographical features for the study of cell migration. *Macromol Biosci* 12(1):12–20
123. Kraning-Rush CM, Califano JP, Reinhart-King CA (2012) Cellular traction stresses increase with increasing metastatic potential. *PLoS One* 7(2):e32572
124. Darling EM, Zauscher S, Block JA, Guilak F (2007) A thin-layer model for viscoelastic, stress-relaxation testing of cells using atomic force microscopy: do cell properties reflect metastatic potential? *Biophys J* 92(5):1784–1791
125. Guck J, Schinkinger S, Lincoln B, Wottawah F, Ebert S, Romeyke M, Lenz D, Erickson HM, Ananthakrishnan R, Mitchell D, Kas J, Ulvick S, Bilby C (2005) Optical deformability as an inherent cell marker for testing malignant transformation and metastatic competence. *Biophys J* 88(5):3689–3698
126. Cross SE, Jin YS, Rao J, Gimzewski JK (2007) Nanomechanical analysis of cells from cancer patients. *Nat Nanotechnol* 2(12):780–783
127. Ramanujan S, Pluen A, McKee TD, Brown EB, Boucher Y, Jain RK (2002) Diffusion and convection in collagen gels: implications for transport in the tumor interstitium. *Biophys J* 83(3):1650–1660
128. Hegedus B, Marga F, Jakab K, Sharpe-Timms KL, Forgacs G (2006) The interplay of cell-cell and cell-matrix interactions in the invasive properties of brain tumors. *Biophys J* 91(7):2708–2716
129. Qazi H, Shi ZD, Tarbell JM (2011) Fluid shear stress regulates the invasive potential of glioma cells via modulation of migratory activity and matrix metalloproteinase expression. *PLoS One* 6(5):e20348
130. Binder DK, Berger MS (2002) Proteases and the biology of glioma invasion. *J Neurooncol* 56(2):149–158
131. Rizvi I, Gurkan UA, Tasoglu S, Alagic N, Celli JP, Mensah LB, Mai Z, Demirci U, Hasan T (2013) Flow induces epithelial-mesenchymal transition, cellular heterogeneity and biomarker modulation in 3D ovarian cancer nodules. *Proc Natl Acad Sci USA* doi: 10.1073/pnas.1216989110
132. Yamada KM, Cukierman E (2007) Modeling tissue morphogenesis and cancer in 3d. *Cell* 130(4):601–610
133. Hutmacher DW (2010) Biomaterials offer cancer research the third dimension. *Nat Mater* 9(2):90–93
134. Feder-Mengus C, Ghosh S, Reschner A, Martin I, Spagnoli GC (2008) New dimensions in tumor immunology: what does 3d culture reveal? *Trends Mol Med* 14(8):333–340
135. Cheema U, Brown RA, Alp B, MacRobert AJ (2008) Spatially defined oxygen gradients and vascular endothelial growth factor expression in an engineered 3d cell model. *Cell Mol Life Sci* 65(1):177–186
136. Orimo A, Gupta PB, Sgroi DC, Arenzana-Seisdedos F, Delaunay T, Naeem R, Carey VJ, Richardson AL, Weinberg RA (2005) Stromal fibroblasts present in invasive human breast carcinomas promote tumor growth and angiogenesis through elevated sdf-1/cxcl12 secretion. *Cell* 121(3):335–348
137. Dong Z, Nor JE (2009) Transcriptional targeting of tumor endothelial cells for gene therapy. *Adv Drug Deliv Rev* 61(7–8):542–553

138. Karnoub AE, Dash AB, Vo AP, Sullivan A, Brooks MW, Bell GW, Richardson AL, Polyak K, Tubo R, Weinberg RA (2007) Mesenchymal stem cells within tumour stroma promote breast cancer metastasis. *Nature* 449(7162):557–563
139. Studebaker AW, Storci G, Werbeck JL, Sansone P, Sasser AK, Tavolari S, Huang T, Chan MW, Marini FC, Rosol TJ, Bonafe M, Hall BM (2008) Fibroblasts isolated from common sites of breast cancer metastasis enhance cancer cell growth rates and invasiveness in an interleukin-6-dependent manner. *Cancer Res* 68(21):9087–9095
140. Kalluri R, Zeisberg M (2006) Fibroblasts in cancer. *Nat Rev Cancer* 6(5):392–401
141. Orimo A, Weinberg RA (2006) Stromal fibroblasts in cancer: a novel tumor-promoting cell type. *Cell Cycle* 5(15):1597–1601
142. Anghelina M, Krishnan P, Moldovan L, Moldovan NI (2006) Monocytes/macrophages cooperate with progenitor cells during neovascularization and tissue repair-conversion of cell columns into fibrovascular bundles. *Am J Pathol* 168:529–541
143. Ceyhan E, Xu F, Gurkan UA, Emre AE, Turali ES, El Assal R, Acikgenc A, Wu CAM, Demirci U (2012) Prediction and control of number of cells in microdroplets by stochastic modeling. *Lab Chip* 12(22):4884–4893
144. Gurkan UA, Sung Y, El Assal R, Xu F, Trachtenberg A, Kuo W, Demirci U (2012) Bioprinting anisotropic stem cell microenvironment. *J Tissue Eng Regen Med* 6:366
145. Xu F, Sridharan B, Wang SQ, Gurkan UA, Syverud B, Demirci U (2011) Embryonic stem cell bioprinting for uniform and controlled size embryoid body formation. *Biomicrofluidics* 5(2)
146. Xu F, Wu JH, Wang SQ, Durmus NG, Gurkan UA, Demirci U (2011) Microengineering methods for cell-based microarrays and high-throughput drug-screening applications. *Biofabrication* 3(3):34101–34113
147. Gurkan UA, Fan Y, Xu F, Erkmen B, Urkac ES, Parlakgul G, Bernstein J, Xing W, Boyden ES, Demirci U (2013) Simple precision creation of digitally specified, spatially heterogeneous, engineered tissue architectures. *Adv Mater* 25(8):1192–1198
148. Sekeroglu K, Gurkan UA, Demirci U, Demirel MC (2011) Transport of a soft cargo on a nanoscale ratchet. *Appl Phys Lett* 99(6)
149. Feng X, JinHui W, ShuQi W, Naside Gozde D, Umut Atakan G, Utkan D (2011) Microengineering methods for cell-based microarrays and high-throughput drug-screening applications. *Biofabrication* 3(3):034101
150. Durmus NG, Tasoglu S, Demirci U (2013) Bioprinting: Functional droplet networks. *Nat Mater* 12(6):478–479.
151. Birgersdotter A, Sandberg R, Ernberg I (2005) Gene expression perturbation in vitro—a growing case for three-dimensional (3d) culture systems. *Semin Cancer Biol* 15(5):405–412
152. Kimlin LC, Casagrande G, Virador VM (2013) In vitro three-dimensional (3d) models in cancer research: an update. *Mol Carcinog* 52(3):167–182
153. Abu-Yousif AO, Rizvi I, Evans CL, Celli JP, Hasan T (2009) Puramatrix encapsulation of cancer cells. *J Vis Exp* (34)
154. Zhong W, Celli JP, Rizvi I, Mai Z, Spring BQ, Yun SH, Hasan T (2009) In vivo high-resolution fluorescence microendoscopy for ovarian cancer detection and treatment monitoring. *Br J Cancer* 101(12):2015–2022
155. Gurski LA, Petrelli NJ, Jia X, Farach-Carson MC (2010) 3d Matrices for anti-cancer drug testing and development. *Oncology* 1(2):20–25
156. Kim J (2005) Three-dimensional tissue culture models in cancer biology. *Semin Cancer Biol* 15:365–377
157. Miller BE, Miller FR, Heppner GH (1985) Factors affecting growth and drug sensitivity of mouse mammary tumor lines in collagen gel cultures. *Cancer Res* 45(9):4200–4205
158. Martin KJ, Patrick DR, Bissell MJ, Fournier MV (2008) Prognostic breast cancer signature identified from 3d culture model accurately predicts clinical outcome across independent datasets. *PLoS One* 3(8):e2994
159. Kunz-Schughart LA, Freyer JP, Hofstaedter F, Ebner R (2004) The use of 3-d cultures for high-throughput screening: the multicellular spheroid model. *J Biomol Screen* 9(4):273–285

160. Hancock JD, Lessnick SL (2008) A transcriptional profiling meta-analysis reveals a core EWS-FLI gene expression signature. *Cell Cycle* 7(2):250–256
161. Teicher BA (2009) Acute and chronic in vivo therapeutic resistance. *Biochem Pharmacol* 77(11):1665–1673
162. Bartholoma P, Reininger-Mack A, Zhang Z, Thielecke H, Robitzki A (2005) A more aggressive breast cancer spheroid model coupled to an electronic capillary sensor system for a high-content screening of cytotoxic agents in cancer therapy: 3-dimensional in vitro tumor spheroids as a screening model. *J Biomol Screen* 10(7):705–714
163. Zhang X, Wang W, Yu W, Xie Y, Zhang X, Zhang Y, Ma X (2005) Development of an in vitro multicellular tumor spheroid model using microencapsulation and its application in anticancer drug screening and testing. *Biotechnol Prog* 21(4):1289–1296
164. Schmeichel KL, Bissell MJ (2003) Modeling tissue-specific signaling and organ function in three dimensions. *J Cell Sci* 116(12):2377–2388
165. Gudjonsson T, Ronnov-Jessen L, Villadsen R, Rank F, Bissell MJ, Petersen OW (2002) Normal and tumor-derived myoepithelial cells differ in their ability to interact with luminal breast epithelial cells for polarity and basement membrane deposition. *J Cell Sci* 115(1):39–50
166. Demirbag B, Huri PY, Kose GT, Buyuksungur A, Hasirci V (2011) Advanced cell therapies with and without scaffolds. *Biotechnol J* 6(12)
167. Drewitz M, Helbling M, Fried N, Bieri M, Moritz W, Lichtenberg J, Kelm JM (2011) Towards automated production and drug sensitivity testing using scaffold-free spherical tumor micro-tissues. *Biotechnol J* 6(12):1488–1496
168. Rodríguez-Dévora JI, Shi Z-d XT (2011) Direct assembling methodologies for high-throughput bioscreening. *Biotechnol J* 6(12)
169. Debnath J, Brugge JS (2005) Modelling glandular epithelial cancers in three-dimensional cultures. *Nat Rev Cancer* 5(9):675–688
170. Yoshida D, Teramoto A (2007) The use of 3-d culture in peptide hydrogel for analysis of discoidin domain receptor 1-collagen interaction. *Cell Adh Migr* 1(2):92–98
171. Cheng K, Lai Y, Kisaalita WS (2008) Three-dimensional polymer scaffolds for high throughput cell-based assay systems. *Biomaterials* 29(18):2802–2812
172. Marrero B, Messina J, Heller R (2009) Generation of a tumor spheroid in a microgravity environment as a 3d model of melanoma. *In Vitro Cell Dev Biol Anim* 45(9):523–534
173. Smith SJ, Wilson M, Ward JH, Rahman CV, Peet AC, Macarthur DC, Rose F, Grundy RG, Rahman R (2012) Recapitulation of tumor heterogeneity and molecular signatures in a 3d brain cancer model with decreased sensitivity to histone deacetylase inhibition. *PLoS One* 7(12)
174. Tang J, Cui J, Chen R, Guo K, Kang X, Li Y, Gao D, Sun L, Xu C, Chen J, Tang Z, Liu Y (2011) A three-dimensional cell biology model of human hepatocellular carcinoma in vitro. *Tumor Biol* 32(3):469–479
175. Becker JL, Blanchard DK (2007) Characterization of primary breast carcinomas grown in three-dimensional cultures. *J Surg Res* 142(2):256–262
176. Taga M, Yamauchi K, Odle J, Furian L, Sundaresan A, Ramesh GT, Pellis NR, Andrassy RJ, Kulkarni AD (2006) Melanoma growth and tumorigenicity in models of microgravity. *Aviat Space Environ Med* 77(11):1113–1116
177. Rhee HW, Zhou HE, Pathak S, Multani AS, Pennanen S, Visakorpi T, Chung LWK (2001) Permanent phenotypic and genotypic changes of prostate cancer cells cultured in a three-dimensional rotating-wall vessel. *In Vitro Cell Dev Biol Anim* 37(3):127–140
178. Chopra V, Dinh TV, Hannigan EV (1997) Three-dimensional endothelial-tumor epithelial cell interactions in human cervical cancers. *Vitro Cellular & Developmental Biology-Animal* 33(6):432–442
179. Qian A, Zhang W, Xie L, Weng Y, Yang P, Wang Z, Hu L, Xu H, Tian Z, Shang P (2008) Simulated weightlessness alters biological characteristics of human breast cancer cell line MCF-7. *Acta Astronaut* 63(7–10):947–958